Journal of Cleaner Production 276 (2020) 124203

Contents lists available at ScienceDirect

Journal of Cleaner Production

journal homepage: www.elsevier.com/locate/jclepro

Synthesis of bio-based polyurethane foam modified with rosin using an environmentally-friendly process

Chu-Chun Hsieh, Yi-Chun Chen*

Department of Forestry, National Chung-Hsing University, 145 Xingda Rd, South Dist, Taichung, 402, Taiwan

ARTICLE INFO

Article history:
Received 7 May 2020
Received in revised form
9 September 2020
Accepted 12 September 2020
Available online 17 September 2020

Handling editor. Cecilia Maria Villas Bôas de Almeida

Keywords:
Caster oil
Environmentally-friendly
Polyurethane
Rosin
Wettability

ABSTRACT

Rosin is mainly composed of abietic acid, which enhances the properties of materials that have a high cost and which involve a complicated process. This study produces high-performance polyurethane (PU) foam at a normal temperature and pressure without the use of a solvent using a simple and environmentally-friendly process. A small amount of rosin is added as a raw functional monomer to modify the PU foam. Castor oil dissolves the rosin and can be used directly as a bio-based polyol. PU foams are prepared from castor oil with 0, 5 and 10% molar ratio rosin as a polyol and isocyanate Desmodur N. The molar ratio of NCO/OH is 1.5 and 2.0. The results show that increasing the molar ratio of rosin increases the density and compressive strength of PU foams. The compressive strength is increased more than three-fold in optimal conditions, which is a better result than previous studies. The wettability results show that the water contact angles of foams are 109°–115°, which dictates the surface is hydrophobic. The water absorption kinetics of foams obey Schott's second-order kinetics and the results verify that adding rosin increases the initial water-aborted rate and decreases water absorption. The solvent resistance results show that the foams have good durability in water and solvents. The patterns for thermogravimetric analysis (TGA) show that a PU foam with a 5% molar ratio of rosin is most thermally stable. The improvement in mechanical and chemical properties is attributed to the hydrophenanthrene ring structure of rosin, and less related to the molar ratio of NCO/OH. This study demonstrates that bio-based PU foams are improved by adding only 2–4 wt% rosin to produce foams with excellent mechanical and chemical properties, controlled water absorption and thermal stability. The results show that this green synthesis process is a viable alternative to current manufacturing processes for high-quality foams.

1. Introduction

PU resin is a commonly available industrial material that is used in the manufacturing of cushioning material, adhesive, coatings, films and composites (Engels et al., 2013). The polymerization of PU involves a reaction with isocyanate and polyol to form a resin with a urethane structure. PU is a candidate to traditional plastic because it is easily processed, with crosslinking and curing at normal/low temperature and pressure, so low energy is required and its good flexibility renders it suited to a wide range of industrial applications (Vale et al., 2019). PU can also be biodegradable and biocompatible (Chien et al., 2017). PU is mainly produced using petrochemical raw materials. These are not renewable so its production increases old carbon reservoirs and causes serious greenhouse effects. The petro-materials can be replaced with bio-based materials to increase the proportion of biomass in PU raw materials (Miao et al., 2014). Bio-based PU resins are renewable raw materials so they are ecologically advantageous (Sheldon, 2012).

Plant oil from crop-derived fats and oils is an important substitute for currently used petro-materials. The plant oil is extracted and refined from seeds or fruit, such as peanuts, soybeans, corn and castor (Meier et al., 2007). Castor (*Ricinus Communis*) is a tropical plant that tolerates drought and which can be used to reclaim land because it grows in barren areas (Babita et al., 2010). The toxic phytotoxin ricin is present in castor beans so the non-edible oil reduces competition with food crops and is mainly used for

* Corresponding author.Tel: +886 4 22840348 #148, Fax: +886 4 22873628
E-mail address: chenyc@nchu.edu.tw (Y.-C. Chen).

https://doi.org/10.1016/j.jclepro.2020.124203
0959-6526/

medicinal and industrial purposes (Mubofu, 2016; Mutlu and Meier, 2010; Sehgal et al., 2010). The main ingredient of castor oil is ricinoleic acid, which has a hydroxyl group that is used directly as a polyol (Chen and Tai, 2018). A previous study showed that 70% of castor oil is exported from India and the remainder from China, Brazil, and Thailand. It also notes that the respective worldwide production of castor seeds and oil are ca. one million tons and ca. 500,000 tons (Ogunniyi, 2006). The supply is stable, so it is a biomass that is widely used in PU industrial raw materials (Mutlu and Meier, 2010).

Rosin is a wood resin that is extracted from *Pinus* or conifers. The components are a variety of rosin acids, such as abietic acid and its isomers. Rosin is an important material for marine waterproofing because abietic acid is hydrophobic (Wilbon et al., 2013). Rosin and its derivatives are commonly used as sizing agents to manufacture water-resistant paper (Wang et al., 1999). The ring structure of abietic acid means that rosin has high thermal stability, with a degradation temperature of more than 350 °C (Tudorachi et al., 2012).

To improve the properties of polymeric materials, fillers or reactants are added to modify physical and chemical properties. Some studies use organic and inorganic filler to enhance the characteristics of polymers (Borisova et al., 2019; Lee et al., 2018). A modified the chemical structure had a positive effect on the properties of polymeric materials. Many studies have reported modified rosin that is used as a polyol to produce PU resin. Zhang et al. (1995) produced maleopimaric acid (MPA) from rosin and then reacted it with linear alkyldiols to produce rosin-based polyol as a raw material for PU foams. Rosin-based polyols affect the thermal stability of PU foams. Jin et al. (2002) synthesized rosin-based polyol using MPA, diethylene glycol, ethylene glycol and the catalysts, phthalic anhydride and adipic acid, in an atmosphere of nitrogen. The results show that the physical properties of rosin-based PU foams are better than those of commercial foams. Zhang et al. (2015) used phosphorus–nitrogen flame retardant to enhance the physical and fire retardant properties of rosin-based PU. Previous studies show that modified rosin can be used as a polyol to synthesize PU foam with improved properties. The hydrophenanthrene ring structure means that rosin produces a PU foam with good compressive strength, thermal stability and dimensional stability. However, rosin costs between 6.6 and 12.6 $/kg in Taiwan. The unstable supply of rosin means that the price fluctuates. Previous studies use three steps to produce a rosin-based polyol (Jin et al., 2002; Zhang et al., 1995, 2015). The cost and the complicated process that is required to produce rosin-based polyol limit the applications of bio-based PU (Centi and Perathoner, 2003).

This study reports the use of castor oil as a polyol and reacts it with isocyanates to produce castor oil-based PU foam and its composite (Chen and Tai, 2018). Castor oil is used as a solvent to dissolve rosin. This study adds a small amount of rosin as a raw functional monomer to modify castor oil-based polyol. To the authors' best knowledge, this study is the first to directly mix castor oil and rosin as a bio-based polyol. The mixture of reactants is synthesized without an organic solvent at room temperature. This is an environmentally-friendly and simple process to produce bio-based PU foams. The synthetic route is shown in Scheme 1. The

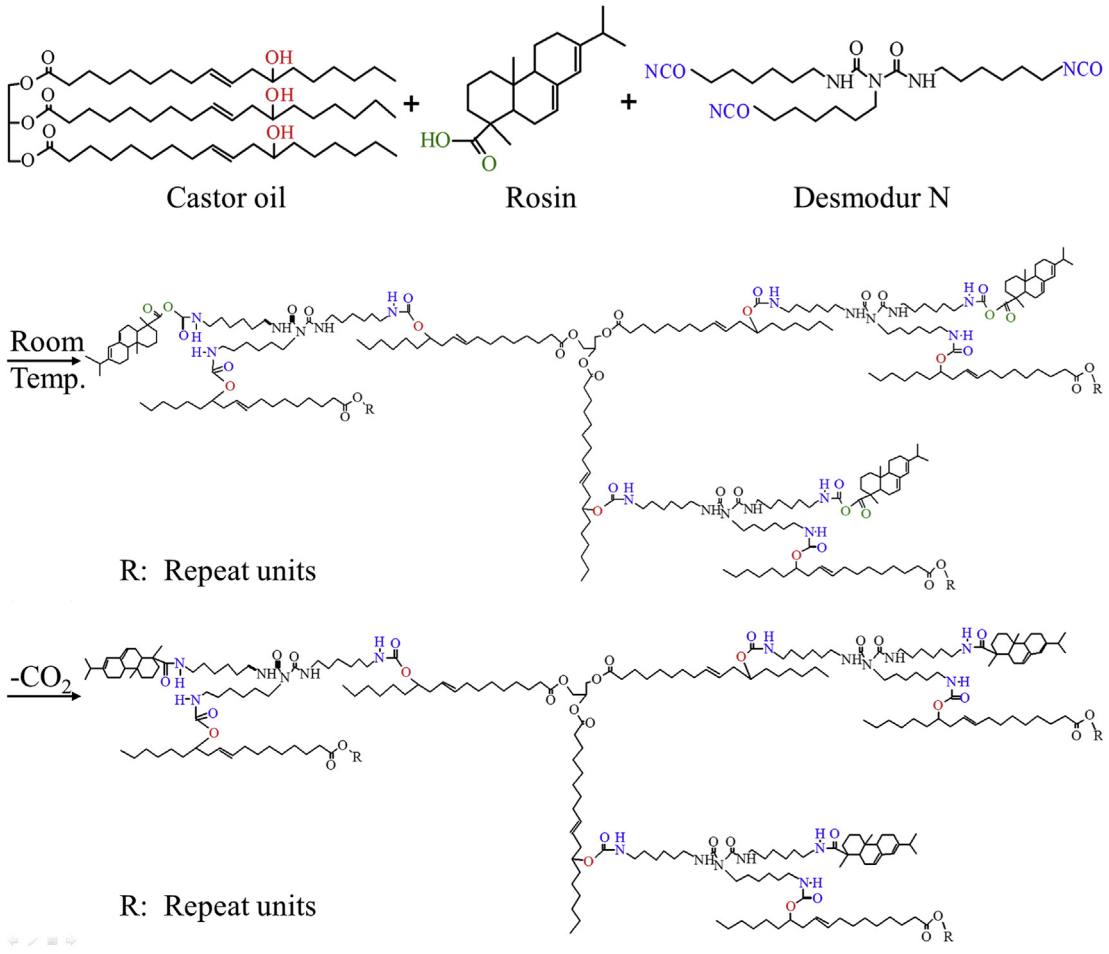

Scheme 1. Chemical synthesis route for castor oil-based PU foam that is modified with rosin.

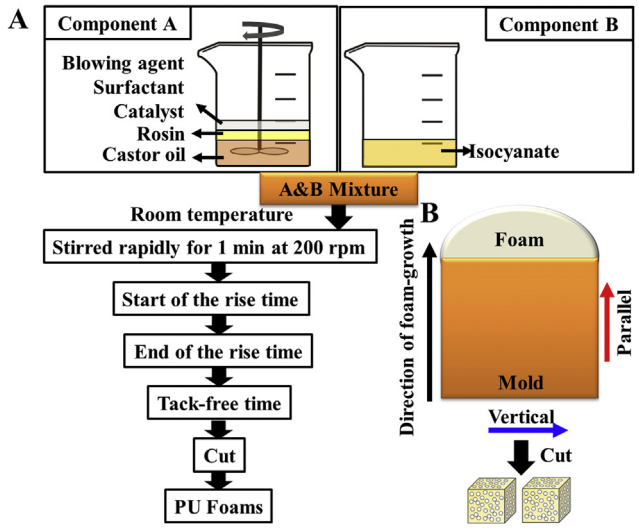

Scheme 2. Flow chart for the preparation of (A) and direction (B) of castor oil-based PU foam that is modified with rosin.

hydroxyl group in castor oil and the carboxylic group in rosin with isocyanate form the urethane (Kashif and Ahmad, 2014) and *N*-carboxylic anhydride structure. Then, the carboxylic group of the structure decomposes and generates amine and CO_2 Stanzione et al. (2018)(Stanzione et al., 2018). The preparation, reactivity, chemical structure, water absorption, solvent resistance, mechanical properties and thermogravimetric behavior of bio-based PU foams are determined in this study.

2. Materials and methods

2.1. Materials

Isocyanate with a solid content of 100%, Desmodur N (Hexamethylene diisocyanate trimer) was purchased from An Fong Develop Co., Ltd., Taichung, Taiwan. The NCO content was 23.07%. Castor oil was purchased from Chung-Hsing Chemical, Taichung, Taiwan. Rosin was obtained from First Chemical Works, Taipei, Taiwan. Rosin, X Grade, is produced in Indonesia. The supplier states that the softening point and the saponification value of rosin are 80 °C and 180 mg KOH/g, respectively. The hydroxyl values for castor oil and rosin are 148.83 and 175.4 mg KOH/g. The blowing agent and surfactant were mixed with distilled water and organosiloxane (DABCO DC5388). The catalyst was dibutyl tin dilaurate (DBTDL; CAS No. 77-58-7) (An Fong Development Co., LTD). Organosiloxane and DBTDL were obtained from Ya Chung Industrial Co., Taiwan. The NCO content and hydroxyl value were determined in the authors' laboratory.

2.2. Basic properties of the raw materials

Castor oil and Desmodur N underwent no pretreatment. Rosin was ground and sieved through a 60-mesh sieve before the experiments. The acid and hydroxyl values for castor oil and rosin and the NCO% for Desmodur N were determined using the standard methods that are descried in a previous study (Lee et al., 2018). The NCO content of isocyanate was calculated using the equation:

$$\text{NCO}\ (\%) = \frac{\text{Weight of NCO group}}{\text{Weight of Desmodur N}} \times 100$$

2.3. Production of PU foam

Scheme 2A shows the flow chart for the preparation of bio-based PU that is modified with rosin. Two mixtures of raw materials were produced to synthesize PU. Component A consisted of polyols that are castor oil-based in a mixture of 0, 5 and 10% rosin, based on the molar ratio of polyol and other agents, including the blowing agent, the surfactant and the catalyst. Component B was isocyanate that is based on component A to produce NCO/OH 1.5 or 2.0 (Table 1). Components A and B were mixed in a cup at room temperature and stirred rapidly for 1 min at 200 rpm. Photographs of the mixture before and after rising are shown in Fig. S1. Similarly to a previous study, the start of the rise time, the end of the rise time and the tack-free time and volume expansion were recorded. These data were used to determine the properties and reactivity of the foam (Chen and Tai, 2018).

2.4. Physical analysis of PU foam

2.4.1. Density

In accordance with ASTM D1622, specimens were cut into 2.54 × 2.54 × 2.54 cm^3 cubes and the volume and weight were measured to calculate the density of specimens. The density is calculated as:

$$\text{Denstiy}\ (\text{Kg}\,/\,\text{m}^3) = \frac{W_o}{V_o}$$

where W_o (mg) and V_o (cm^3) are the weight and volume of the dry specimens, respectively. Five specimens were measured for this experiment.

Table 1
The weight of the raw materials that are used to produce PU foam.

Code	Weight (parts by weight)					
	Component A					Component B
	Polyol		Blowing agent	Surfactant	Catalyst	Isocyanate
	Castor oil	Rosin				
D1-0[a]	100	0	6	6	6	72.4
D1-5	95.7	4.3	6	6	6	73.0
D1-10	91.4	8.6	6	6	6	73.7
D2-0	100	0	6	6	6	96.5
D2-5	95.7	4.3	6	6	6	97.2
D2-10	91.4	8.6	6	6	6	98.0

[a] The first number 1 or 2 denotes a NCO/OH ratio of 1.5 or 2.0 and the second number denotes the addition of 0, 5 and 10% rosin, based on the OH mole.

2.4.2. FT-IR spectroscopy

The effect of changing the ratio of rosin and NCO/OH ratio on the bonding or group of PU foam was determined using Attenuated total reflectance-Fourier-transform infrared spectroscopy (ATR-FTIR; PerkinElmer spectrum 100) by attenuated total reflectance. The functional groups of the specimens were tested within a spectral range in 650–4000 cm^{-1} at a resolution of 4 cm^{-1}.

2.4.3. Optical micrograph

The images were acquired using a USB digital microscope (UPMOST/UPG629).

2.4.4. Water absorption and kinetics characteristics

In accordance with ASTM C272/C272 M-18, specimens were cut into 2 × 2 × 2 cm^3 cubes and dried over-night in an oven at 60 °C. The specimens were immersed in distilled water at 25 °C and removed at specific time intervals and wiped surface. They were then weighed. This process was repeated for one week. Water absorption was calculated as:

$$\text{Water absorption (At; g/g)} = \frac{W_t - W_o}{W_o}$$

where W_t and W_o are the weight of the water-aborted specimens at time intervals and dry specimens, respectively. Three specimens were measured for this experiment.

Previous research shows that a polymer swells in accordance with Schott's second-order kinetics (Chen and Chen, 2019). This study uses the kinetics model to fit the water-aborted behavior. This kinetics model was used in a previous study to calculate the swelling kinetics of PU composite hydrogels (Huang et al., 2013). The kinetic model is described as (Schott, 1992):

$$\frac{dA_t}{dt} = K(A_t - A_\infty)$$

where A_∞ is the theoretical equilibrium At (g/g) for a second-order kinetic and, K is the specific rate constant for the initial water-aborted rate. The equation is integrated between the limits A_t is 0 when t is 0 and A_t for t. Rearrangement yields the Schott's equation for second-order water-aborted:

$$\frac{t}{A_t} = \frac{1}{KA_\infty^2} + \frac{t}{A_\infty}$$

OriginPro8 was used to calculate the K value and to determine the correlation coefficients (R^2).

2.4.5. Resistance to water and solvents

Specimens with dimensions of 1 × 1 × 1 cm^3 were immersed in 600 mL of distilled water at 25 °C and 50 °C and into acetone, ethyl acetate and toluene and stirred at 200 rpm for 1 h. They were then dried overnight in an oven at 60 °C. Weight retention is calculated as:

$$\text{Weight retention (\%)} = \frac{W_r - W_o}{W_o} \times 100$$

where W_r and W_o are the weights of the treated and the dried specimens, respectively. Five specimens were measured for this experiment.

2.4.6. Wettability

The method follows ASTM C365-00. The wettability of the surface is a goniometer (FACE/CA-D) that is used to measure the

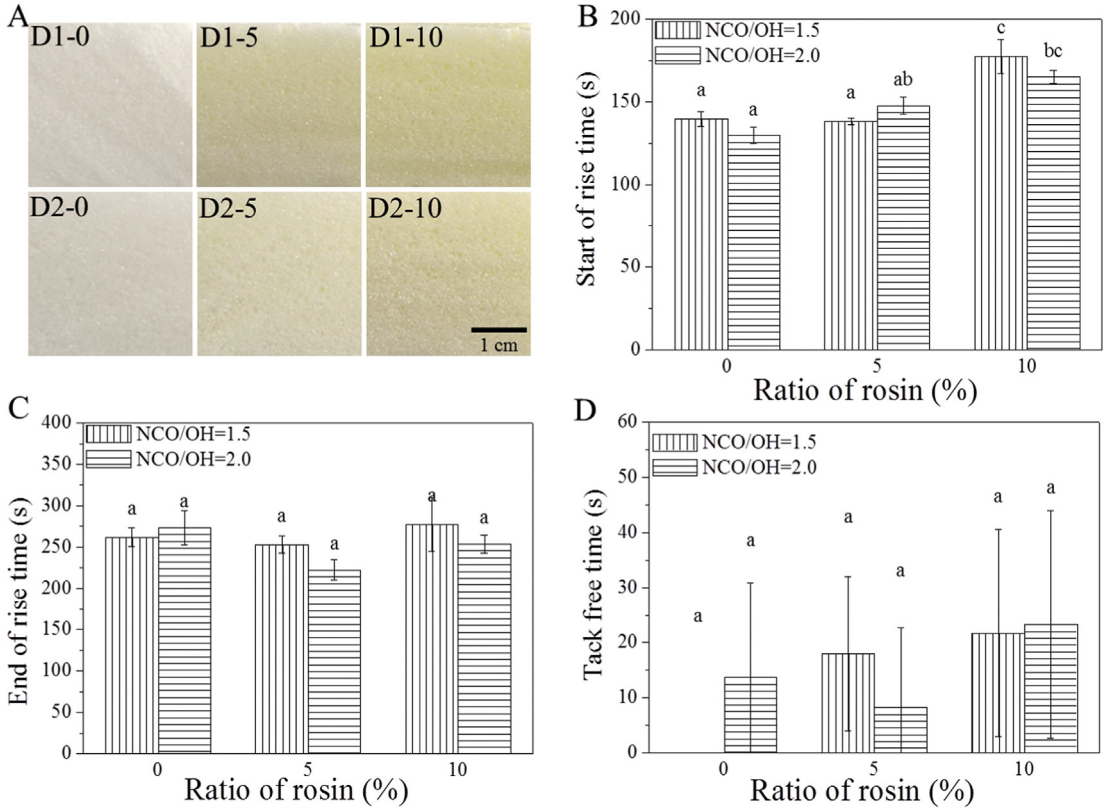

Fig. 1. Appearance (A), Start of rise time (B), end of rise time (C), and tack free time (D) of PU foams. When tack free time was same with end of rise time that was marked as 0 s. For codes D-x-y, the first number, 1 or 2, denotes a NCO/OH ratio of 1.5 or 2.0 and the second number denotes the addition of 0, 5 or 10% rosin, based on the OH mole.

contact angle between deionized water with a 2 mm diameter and the surface of the PU foam at room temperature. The contact angle is given as an average value for 20 drops.

2.4.7. Equilibrium moisture content (EMC)

Specimens were cut into 1 × 1 × 1 cm^3 sections and air-dried at 25 °C for 7 days. The specimens were dried overnight in an oven at 60 °C. The EMC is calculated as:

$$\text{EMC}\ (\%) = \frac{(W_A - W_o)}{W_o} \times 100$$

where W_A and W_o are the weight of the air-dried specimens and the oven-dried specimens, respectively. Three specimens were measured for this experiment.

2.5. Mechanical properties

The method follows ASTM C365-00. Samples were cut into 2.54 × 2.54 × 1.27 cm^3 specimens. The compressive strength was measured vertical and parallel to the foaming direction (Scheme 2B). The mechanical test used a strength testing machine (Shimadzu EZ -500NSX) with a load speed of 5 mm/min. The model number and the capacity of the load cell are SM-500N-168 and 500 N, respectively. The mechanical properties correspond to a stress of 10 and 25% strain and a strain of 2 kPa stress. The improvement in the mechanical properties and compressive strength is calculated as:

$$\text{Improvement of compressive strength performance (times)} = \frac{\sigma_1}{\sigma_0}$$

where σ_1 and σ_0 are the compressive strength of the treated and control groups for stress at 10% strain parallel to the rise direction of the foam. Three specimens were measured for this experiment.

2.6. Thermogravimetric analysis

Thermogravimetric analysis (TGA, PerkinElmer PyrisI) used a heating rate of 10 °C/min from 50 °C to 600 °C in a nitrogen atmosphere to determine the thermal stability of PU foams.

2.7. Statistical analyses

Statistical analysis used SPSS software version 20 (SPSS Inc., Chicago, IL, USA). Scheffe's test was used to determine the statistical significance between data. The P value is 0.05. Letters mark significant differences in the table and the bar graph.

3. Results and discussion

3.1. The basic properties of PU foam

A previous study by the authors manufactured castor oil-based PU foams without solvents at room temperature (25 °C) and at a standard atmospheric pressure (Chen and Tai, 2018). Fig. 1A shows PU foams that are homogeneous. These castor oil-based PU foams with rosin were produced using the same environmentally-friendly process. As the ratio of rosin increases, the PU foams become yellower than the D1-0 and D2-0. Fig. 1B–D shows the foaming behavior for castor oil-based PU foams with rosin. The NCO/OH ratio of the product does not have a significant effect on the results. The results show that the OH group of castor oil reacts with

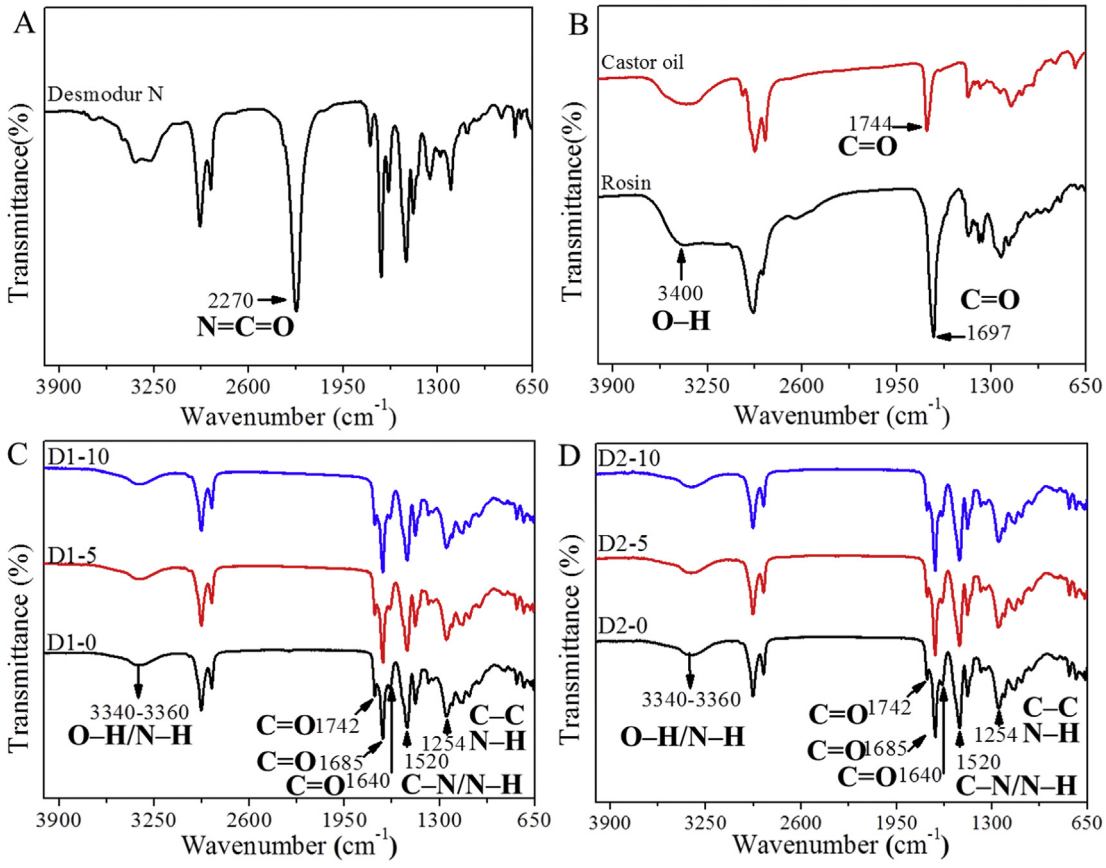

Fig. 2. FT-IR spectra of Desmodur N (A), castor oil (B), rosin and PU foams (C–D).

Table 2
Relative intensity of bonding-urethane, urea and amide to urethane.

Code	Relative absorption intensity[a]			
	Bonded- urethane/urethane (1685 cm^{-1}/ 1742 cm^{-1})	Urea/urethane (1640 cm^{-1}/ 1742 cm^{-1})	Amide II/urethane (1520 cm^{-1}/ 1742 cm^{-1})	Amide III/urethane (1254 cm^{-1}/ 1742 cm^{-1})
D1-0	2.341	0.754	1.985	1.625
D1-5	4.704	0.558	3.763	2.923
D1-10	3.904	0.576	3.148	2.388
D2-0	3.862	1.274	3.382	2.406
D2-5	3.716	1.269	3.260	2.400
D2-10	3.993	1.285	3.474	2.525

[a] Based on the absorption intensity of the urethane bond at 1742 cm^{-1}.

isocyanate quickly, which is similar to the results of a previous study (Chen and Tai, 2018). As the rosin ratio increases, the start of the rise time changes from 139.7 to 177.3 s for a NCO/OH ratio of 1.5. These results show that the NCO group is more reactive with the OH than with the COOH group of rosin. A previous study also shows that NCO groups are more reactive with an OH group than with a COOH group (Jhon et al., 2001). The end of the rise time and the tack-free time show no significant change. The total reaction time for PU foams is ca. 6 min, which reduces the time that is required for manufacturing.

3.2. FTIR spectra for PU foams

Fig. 2 shows FT-IR spectra in the range 650–4000 cm^{-1} for PU foams and their raw materials to compare the structure. In Fig. 2A, the peak at 2270 cm^{-1} is assigned to the NCO group of isocyanate. Castor oil and rosin show a broad OH band between 3630 and 3150 cm^{-1} (Fig. 2B). A peak for rosin at 1697 cm^{-1} is attributed to the C=O stretching vibrations of COOH. The raw materials have similar patterns to those of previous studies (Chen and Tai, 2018; Moustafa et al., 2017). Fig. 2C–D shows that all PU foams have similar patterns and show the same characteristic absorption peaks with castor oil-based PU resin (Chen and Tai, 2018; Gurunathan et al., 2015). An overlap band at 3360-3340 cm^{-1} is attributed to the N–H and O–H stretching vibration. The bands are split into two peaks at 2929 cm^{-1} and 2857 cm^{-1}, which are assigned to the CH_2 and CH_3 groups (Gradinaru, 2012). The results show no absorption peak for the NCO group at 2270 cm^{-1} and isocyanate reacts completely during the reaction (Fig. 2A). The peaks at 1742, 1685 and 1640 cm^{-1} are respectively attributed to the C=O stretching

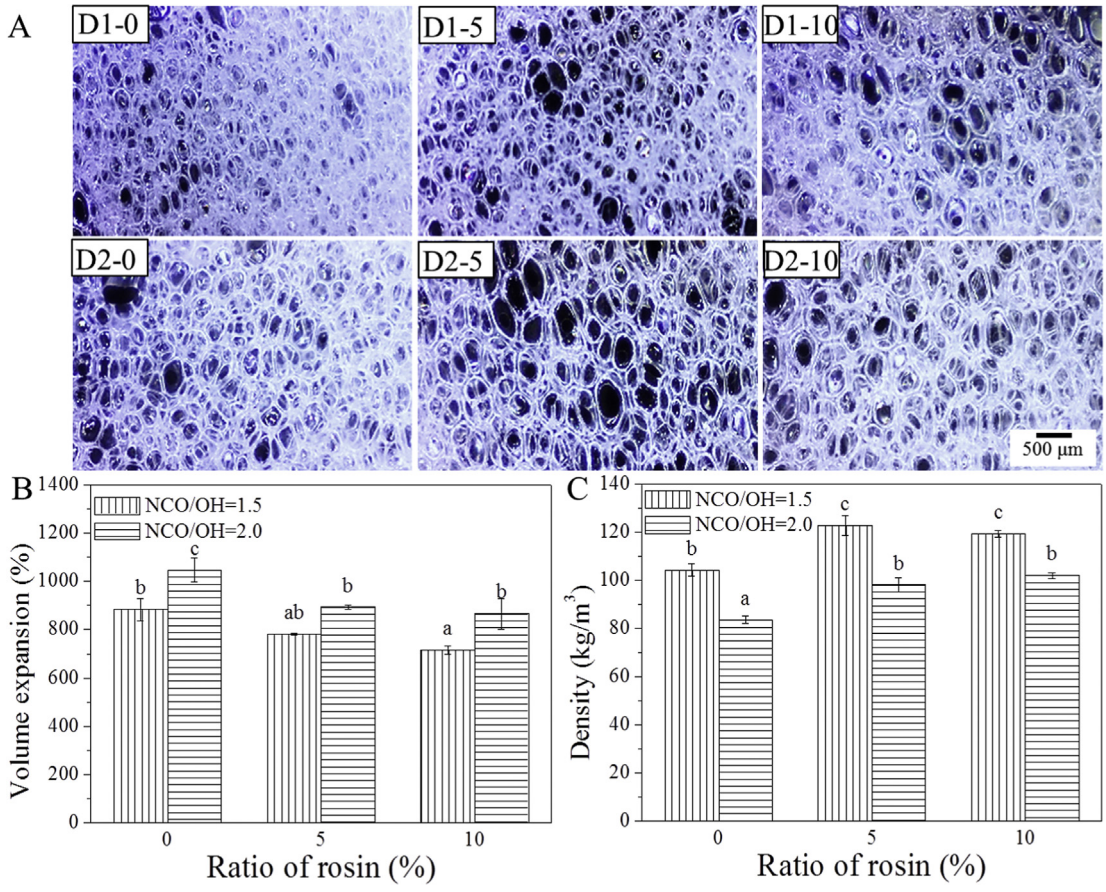

Fig. 3. Pore structure (A), volume expansion (B) and density (C) of PU foams.

vibrations of urethane, bonding-urethane and urea. The N–H bending vibration and the C–N stretching vibration for amide II are both located at 1520 cm^{-1}. The scissoring vibration for CH_2 is located at 1466 cm^{-1}. At 1254 cm^{-1}, there is a characteristic peak for amide III. The relative absorption intensities for bonding-urethane, urea, amide II and amide III to urethane are listed in Table 2. The bonding-urethane peak is more intense than that for free-urethane because the NCO/OH ratios >1. These results show that the higher the NCO/OH ratio, the greater is the ratio of amide II, amide III and urea structures. The long-chain polyol and isocyanate units form soft and hard segments, respectively (Korley et al., 2006). A higher NCO/OH ratio also results in an increase in hard segment content, so the absorption intensity of bonding-urethane increases (Lin and Lee, 2017). A higher rosin ratio results in an increase in amide II and amide III structure for a ratio of NCO/OH ratio of 1.5 because of the reaction between NCO and COOH. For a NCO/OH ratio of 2.0, the ratios of the absorption intensities are slightly different. These results show that the characteristic absorption peaks of NCO/COOH and NCO/OH overlap. A specific ratio of NCO/OH and rosin affects the structure of polymerized urethane.

3.3. Pore structure and density of PU foams

The pore structure, the expansion in volume and the density of PU foams are shown in Fig. 3. Fig. 3A shows PU foams with a homogenous and open-pore structure. The respective density of D1-0, D1-5, D1-10, D2-0, D2-5 and D2-10 is 106.0, 125.3, 124.6, 87.9, 104.4 and 106.1 kg/m^3. These results in Fig. 3B and C shows that a greater NCO/OH ratio results in an increase in the pore size and the volume expansion and a decrease in the density. A higher isocyanate

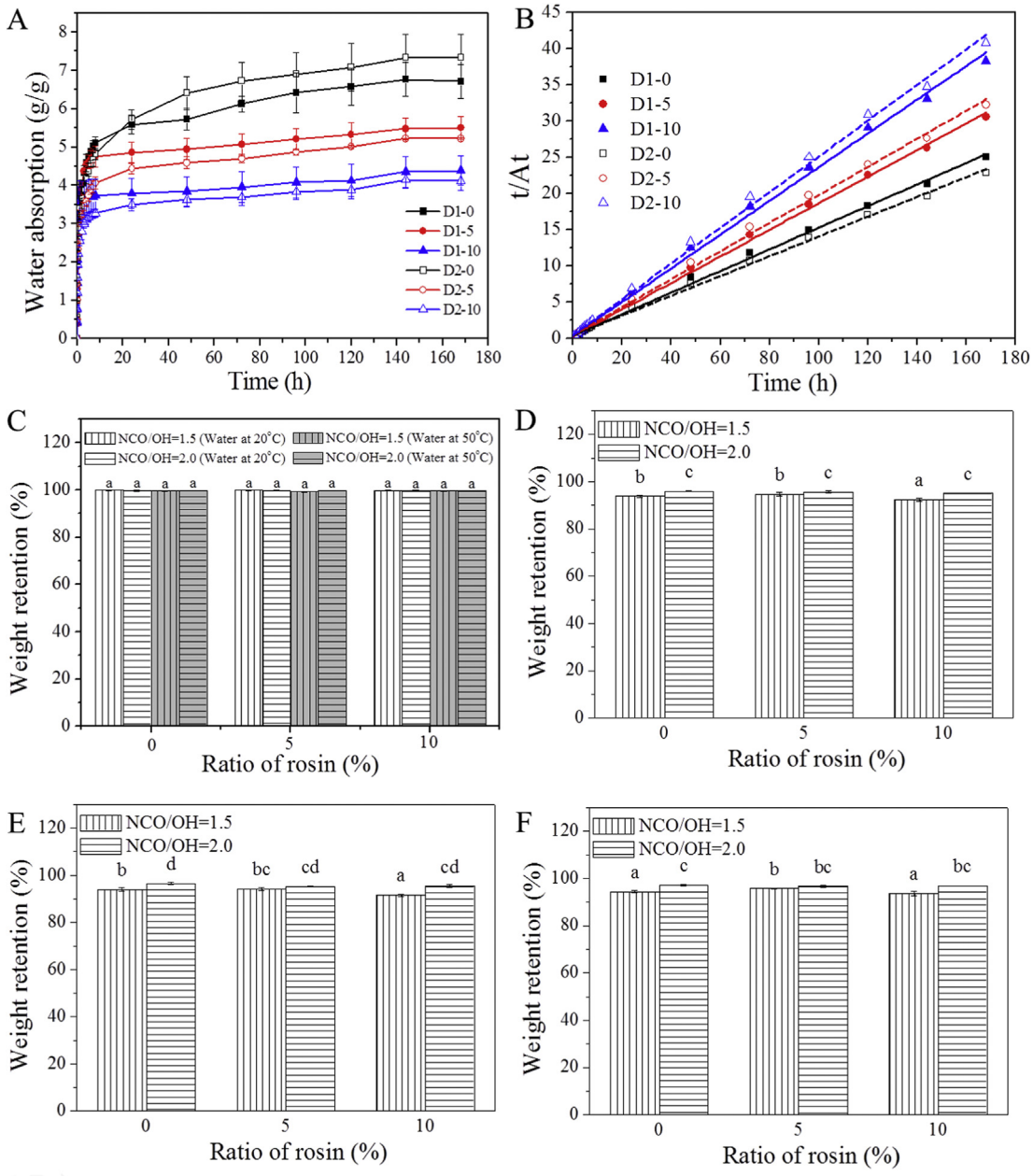

Fig. 4. (A) The absorption of water by PU foams in deionized water at 25 °C and (B) Variation in the reciprocal of the water-aborted rate t/At as a function of the water-aborted time for PU foams. The weight retention of PU foams that are immersed in distilled water (C), acetone (D) ethyl acetate (E) and toluene (F) for 1 h.

content results in an increase in the degree of crosslinking (Semsarzadeh and Navarchian, 2003) and an increase in the release of CO_2 gas for foaming. These results also show that an increase in the rosin content results in a lower volume expansion and a higher density than D1-0 and D2-0. Rosin is a sustainable tackifying agent in resin so the viscosity of the reacting mixture is increased (Lang et al., 2019). There is no change in the volume or the density if rosin was increased from 5 to 10%. The results show that there is an increase in the amount of gas that is generated by the reaction of rosin with isocyanate (Scheme 1). In the first step, the COOH group and the isocyanate form an *N*-carboxylic anhydride structure and CO_2. Subsequently, the *N*-carboxylic anhydride structure reacts and the carboxylic group decomposes and generates amine and CO_2. The amine reacts with the *N*-carboxylic anhydride to produce amine and CO_2 (Stanzione et al., 2018). The gases and the addition of rosin result in low foaming and a smaller increase in volume. The density of specimens is approximately 90–120 kg/m^3 so these are classified as low-density foams (Shi et al., 2006; Singhal et al., 2012). The pore size and density of bio-based PU foams is adjusted by varying the NCO/OH and the rosin molar ratio.

3.4. Water absorption kinetics, wettability and EMC for PU foams

Fig. 4A shows the water absorption curves for PU foam. Water absorption for all specimens samples increases rapidly before 8 h. The respective At values of D1-0, D1-5, D1-10, D2-0, D2-5 and D2-10 are 5.6, 3.8, 4.4, 5.7, 4.9 and 3.5 g/g at 24 h. The NCO/OH ratio and density have no effect on water absorption. Water absorption decreases as the molar ratio of rosin increases. Previous studies show that the At values of castor oil and polyethylene glycol (PEG)-based PU foams are 5.4–15.1 g/g at 40 min (Wang et al., 2015). The At value for rosin-modified PU foams is less than those for castor-oil and/or PEG-based foams. Fig. 4B shows the curves for t/At versus t as straight lines with linear correlation coefficients. Schott's second order kinetics model describes the water absorption into pores of PU foams. Table 3 lists the values for contact angle, EMC and absorption kinetic parameters A_∞, K and the R^2. The value for R^2 confirms the reliability of the model. The results show that the water contact angle for PU foams is 109°–115° and the characteristic values for hydrophobic behavior are similar to those for a previous study (Santos et al., 2017). The EMC for PU foams is less than 0.6%, which also confirms the hydrophobic properties. Increasing NCO/OH and the rosin molar ratio results in a slight decrease in the EMC. Increasing the molar ratio of rosin produces a decrease in A_∞ and an increase in K. These results are due to the pore structure and the hydrophenanthrene ring structure of PU foam that is modified using rosin (Gwon et al., 2016; Wang et al., 2011). A high initial water-aborted rate and low water absorption increase stability in a very humid atmosphere or in aqueous solution. To the authors' best knowledge, this is the first case of Schott's second order kinetics model being used to describe the water absorption behavior of PU foams.

Table 3
Contact angle, EMC and water absorption kinetic parameters for PU foams in terms of the second-order kinetic model.

Code	Contact angle (°)	EMC (%)	A_∞ (g/g)	K × 10^3 (g/g/h)	R^2
D1-0	115.0 ± 4.8^a	0.60 ± 0.03^c	6.6881	7.9	0.9981
D1-5	113.0 ± 3.2^a	0.59 ± 0.04^c	5.4283	15.9	0.9989
D1-10	109.1 ± 6.3^a	0.47 ± 0.03^b	4.2843	20.0	0.9979
D2-0	110.0 ± 3.9^a	0.55 ± 0.03^{cb}	7.3089	5.3	0.9980
D2-5	115.8 ± 4.5^a	0.48 ± 0.04^b	5.1499	11.2	0.9981
D2-10	110.0 ± 2.6^a	0.36 ± 0.02^a	4.0483	15.9	0.9977

3.5. Resistance of PU foams to water and chemicals

Fig. 4C–F shows the weight retention for PU foams in water and solvents. The weight retention for all specimens is approximately 100% in water at 25 °C and 50 °C (Fig. 4C). The results demonstrate that bio-based PU foams are resistant to water. The respective values for weight retention for PU foams are 92.4–96.0%, 91.5–96.5% and 94.4–97.1% in acetone, ethyl acetate and toluene (Fig. 4D–F). The results show that PU foams with a NCO/OH ratio of 2.0 are very resistant to chemicals, as shown by the weight retention in organic solvents, because of the degree of crosslinking. The water retention values for PU resins decreases as the rosin ratio increases. PU is difficult to recycle because it is not biodegradable (Zia et al., 2007). Rosin allows solvent to penetrate into the crosslinked structure so it allows PU to degrade.

3.6. Mechanical properties of PU foams

The vertical and horizontal direction of PU foams shows the rise direction during foam formation. Fig. 5 shows the stress-strain curves for PU foams. There is greater compressive stress in the vertical direction (Fig. 5A–B) than in the horizontal direction (Fig. 5C–D). For press-free foam production, the pores of PU foam extend lengthwise in the foaming direction, which leads to anisotropy. The results are similar to those of a previous study which showed that anisotropy in foams enhances the mechanical properties (Hamilton et al., 2013). Table 4 shows the compressive strength of PU foams at 10% and 25% strain. The results show that compressive strength increases as the NCO/OH, the molar ratio of rosin and strain increase. A high NCO/OH ratio increases the hard segment content and crosslinking (Wadekar et al., 2019) and generates a greater degree of crosslinking, which limits slipping between the chains and enhances the mechanical properties (Huang and Zhang, 2002; Petrović et al., 2002). In the vertical direction, the respective strain values for D1-0, D1-5, D1-10, D2-0, D2-5 and D2-10 are 11.2, 8.1, 9.9, 10.4, 8.5 and 8.1% at 2 kPa. The addition of a 5% molar ratio of rosin for a polyol increases the compressive strength and stiffness of the PU foams significantly. The phenanthrene structure of rosin stiffens the polymer structure (Zhang et al., 1996). Previous studies show that a high-density PU foam has better mechanical properties than a low-density sample (Dhaliwal et al., 2018; Zhang et al., 2019). A low ratio of rosin produces a low-density bio-based PU foam (Fig. 3C) with good mechanical properties.

3.7. Thermal stability of PU foams

The thermal stability of the PU foams is determined using a TGA to scan from 50 °C to 600 °C and a heating rate of 10 °C/min. Fig. 6 shows the TGA and differential thermogravimetric (DTG) curves for PU foams. The TG curves for D1-5 and D2-5 apply to a higher temperature area between 250 and 350 °C than D1-0 and D2-0, as shown in Fig. 6 A and B. This result shows that the addition of a 5% molar ratio of rosin for polyol increases the thermal stability of PU foams. The DTG curves (Fig. 6 C and D) show that the thermal degradation of PU foams occurs in three stages. The respective onset temperature for the first and second stages is 251–260 °C and 395–425 °C. The first stage involves the degradation of the hard components such as urethane (200 °C) and urea (250 °C). The second stage involves the degradation of the soft castor oil component (Hablot et al., 2008). The third stage begins at 491–537 °C and involves the decomposition of the residual compounds. The thermal degradation data for the three stages is listed in Table 5. Most weight is lost (54.1–66.2%) in the first stage.

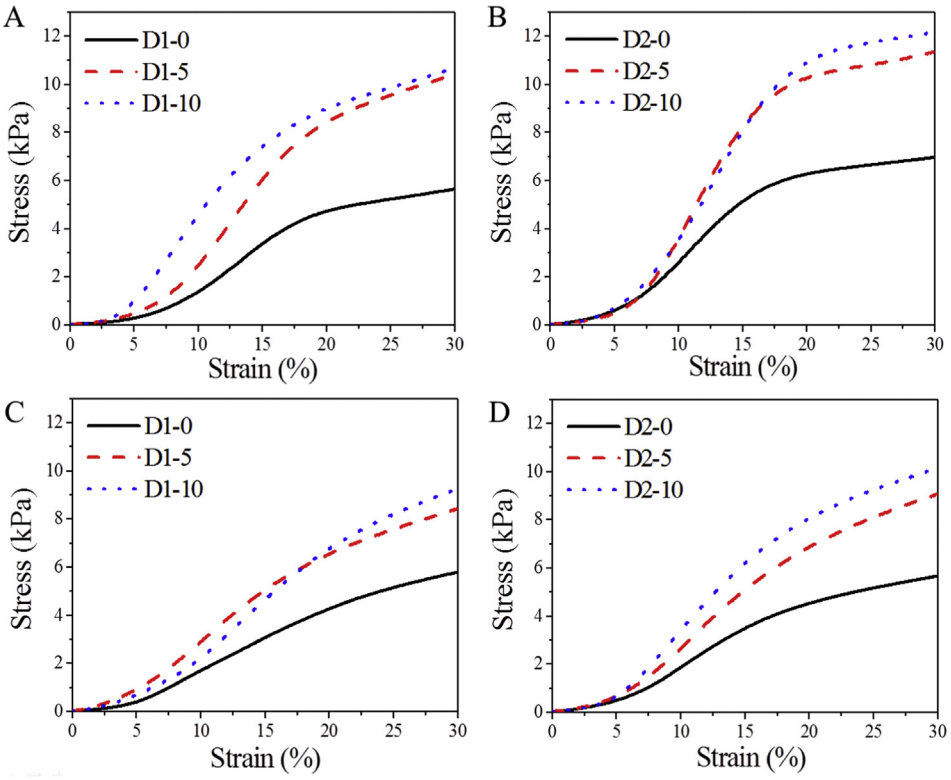

Fig. 5. Stress-strain curves for PU foams parallel (A–B) and vertical (C–D) to the load direction.

Table 4
Compressive strength of PU foams.

Code	Direction[a]	Compressive strength (kPa)		Strain (%) (2 kPa)
		At 10% strain	At 25% strain	
D1-0	Vertical	1.7 ± 0.3^{a}	5.0 ± 0.3^{a}	11.2 ± 0.8^{c}
D1-5		2.9 ± 0.2^{cd}	7.8 ± 0.2^{b}	8.1 ± 0.5^{a}
D1-10		2.1 ± 0.5^{abc}	8.2 ± 0.4^{b}	9.9 ± 1.2^{abc}
D2-0		1.9 ± 0.1^{ab}	5.1 ± 0.1^{a}	10.4 ± 0.2^{bc}
D2-5		2.7 ± 0.1^{bcd}	8.1 ± 0.1^{b}	8.5 ± 0.3^{ab}
D2-10		3.4 ± 0.4^{d}	9.4 ± 0.1^{c}	8.1 ± 0.4^{a}
D1-0	Parallel	1.5 ± 0.3^{a}	5.8 ± 0.5^{a}	10.2 ± 1.3^{b}
D1-5		2.5 ± 0.2^{ab}	9.5 ± 0.4^{c}	8.6 ± 0.7^{ab}
D1-10		4.5 ± 0.5^{c}	9.8 ± 0.3^{cd}	6.8 ± 0.6^{a}
D2-0		2.8 ± 0.3^{b}	6.9 ± 0.4^{b}	10.6 ± 0.7^{b}
D2-5		3.2 ± 0.4^{b}	10.8 ± 0.2^{de}	9.0 ± 0.6^{ab}
D2-10		4.6 ± 0.3^{c}	11.8 ± 0.03^{e}	7.7 ± 0.6^{a}

[a] Rising direction during foam formation (Scheme 2).

During the first stage, increasing the NCO/OH and rosin ratio results in increased weight loss and a higher peak because a high NCO/OH ratio (>1) causes a secondary reaction and forms biuret and allophanate structures, which have low thermal stability (Chattopadhyay and Webster, 2009). The main decomposition temperature of rosin varies from 90 to 450 °C (Yang et al., 2011). During the third stage, increasing the rosin molar ratio results in an increase in the onset/peak temperature and a decrease in the weight loss. This result shows that rosin renders the structure that is formed by the cross-linking reaction of COOH and NCO and the phenanthrene structure more thermally stable (Tudorachi et al., 2012). The temperatures for 10% weight loss for D1-0, D1-5, D1-10, D2-0, D2-5 and D2-10 are 271, 280, 277, 268, 277 and 270 °C, respectively. A 5% molar ratio for rosin in a polyol increases the thermal stability of PU foams over that for a molar ratio of rosin in polyol of zero or 5% because the addition of excess rosin, which is amorphous, with a low molecular weight and is mono-functional, inhibits chain growth and/or crosslinking (Maiti et al., 1989; Tudorachi et al., 2012). The temperature for 30% weight loss is also similar to that for 10% weight loss. The results show that a lower rosin content (ca. 2%) increases thermal stability. Table 6 shows the properties of castor oil and rosin-based PU foams for a previous study. The comparison shows that adding rosin increases thermal stability and this study increases the compressive strength more than previous studies. To reduce the price fluctuations for rosin and side products from the synthesized process, less rosin must be added. The results show that 2–4 wt% rosin in bio-based PU resin improves the thermal and mechanical properties. The synthesis process does not use a solvent at room temperature and uses normal atmospheric pressure, which reduces the energy that is required and the cost. The results show that the process is cost-effective and environmentally-friendly.

4. Conclusion

This study uses rosin as a raw functional monomer to modify castor oil-based PU foams. The single-step process allows the manufacture of bio-based PU foams at room temperature and pressure without the use of solvent. The addition of rosin and NCO/OH affects the chemical structure and increases the hard segment. Rosin-modified PU foams have low-density, low water absorption, high initial water-aborted rate and excellent chemical stability. This is the first study to use Schott's second-order kinetics model to describe the absorption of water into pores in the structure of PU foams. The addition of rosin significantly enhances the mechanical

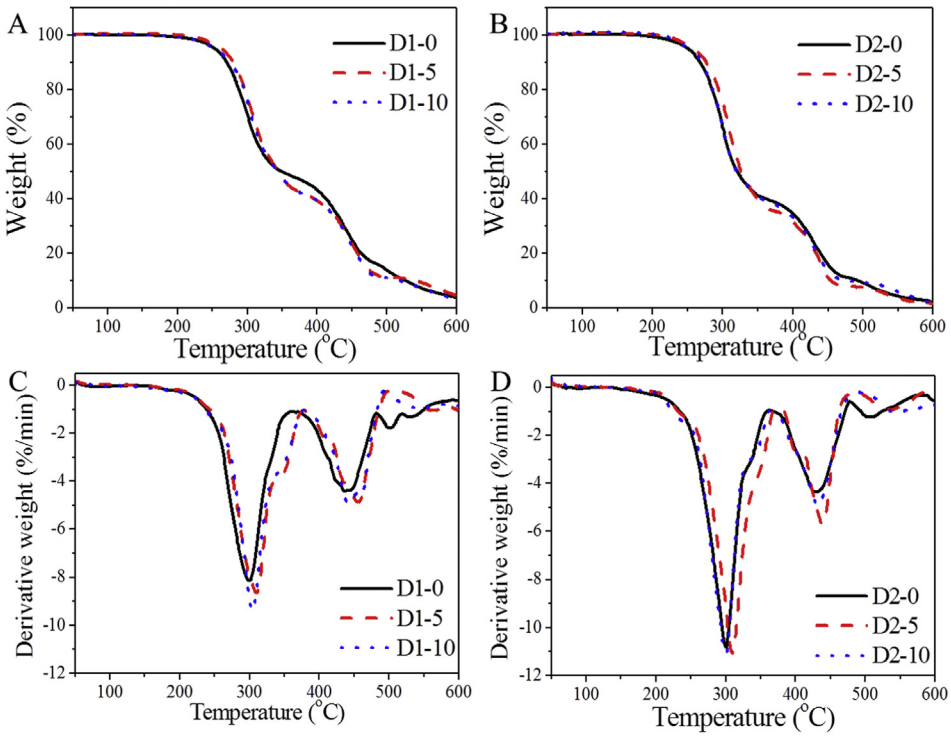

Fig. 6. TGA (A and B) and DTG (C and D) curves for PU foams.

Table 5
Thermal analysis of PU foams.

Code	Stage												T_{10}*3 (°C)	T_{30}*4 (°C)	Char yield *5 (%)
	1				2				3						
	Onset (°C)	Peak (°C)	WL*1 (%)	PH*2 (%/min)	Onset (°C)	Peak (°C)	WL (%)	PH (%/min)	Onset (°C)	Peak (°C)	WL (%)	PH (%/min)			
D1-0	251	299	54.1	8.1	397	437	29.1	4.4	491	501	8.7	1.8	271	301	3.6
D1-5	260	310	60.4	8.6	425	457	27.4	4.8	537	564	8.2	1.0	280	309	4.4
D1-10	262	304	60.8	9.40	415	441	26.8	5.0	510	544	5.2	1.0	277	307	3.0
D2-0	255	300	62.9	10.8	395	428	26.5	4.4	492	506	6.7	1.2	268	297	2.1
D2-5	259	309	66.2	11.0	401	439	26.2	5.7	504	534	5.2	0.9	277	306	1.5
D2-10	253	300	63.8	11.0	397	432	26.2	4.9	514	545	4.3	1.0	270	297	1.7

*1 wt loss.
*2Peak height.
*3Temperature of 10% weight loss.
*4Temperature of 30% weight loss.
*5 wt retention at 600 °C.

Table 6
The comparison of properties of bio-based PU foams.

Bio-based Polyol	Modified agent	Density (Kg/m^3)	Thermal stability	Improvement of compressive strength performance (times)	Reference
Castor oil	Rosin	87.9–125.3	Increase	3.07	This study
	Glycerol or pentaerythritol	37.5–38.3	Decrease	1.15	Zhang et al. (2014)
	Polyglycerol	46.5–47.3	Decrease	1.88	Hejna et al. (2017)
	Phosphate	36.9–37.2	Increase	0.91	Zhang et al. (2013)
	Soy protein	63–91	Decrease	1.41	Zhang et al. (2018)
Rosin	Maleopimaric anhydride	36.8–37.0	Increase	1.12	Jin et al. (2002)
	Maleopimaric anhydride/Aniline	43.8–48.4	Increase	1.2	Zhang et al. (2015)

and thermal properties of PU foams. The compressive strength of rosin-modified PU foam is increased more than three-fold in optimal conditions. The results show that a 5% molar ratio of rosin in a polyol is the optimal concentration. This study demonstrates that the addition of less rosin material enhances the properties of bio-based PU foam with a hydrophenanthrene ring structure. This study offers a simple, environmentally and low-cost strategy to manufacture high-quality PU foams that reduces pollution.

CRediT authorship contribution statement

Chu-Chun Hsieh: Formal analysis, Software, Methodology, Visualization, Validation, Data curation, Writing - original draft, Visualization. **Yi-Chun Chen:** Funding acquisition, Supervision, Visualization, Project administration, Resources, Writing - review & editing, Conceptualization, Methodology, Project administration, Writing - review & editing.

Declaration of competing interest

The authors declare that they have no known competing financial interests or personal relationships that could have appeared to influence the work reported in this paper.

Acknowledgements

This work was supported by Ministry of Science and Technology of Taiwan (ROC) (107-2311-B-005-010-MY3 and 108-2813-C-005-069-B). Prof. Wen-Jau Lee (Department of Forestry, National Chung Hsing University) kindly provided experimental support and this is much appreciated. The authors would like to thank Ms. Mei-Ying Chiu for inspiring this study.

Appendix A. Supplementary data

Supplementary data to this article can be found online at https://doi.org/10.1016/j.jclepro.2020.124203.

References

Babita, M., Maheswari, M., Rao, L.M., Shanker, A.K., Rao, D.G., 2010. Osmotic adjustment, drought tolerance and yield in castor (Ricinus communis L.) hybrids. Environ. Exp. Bot. 69, 243–249. https://doi.org/10.1016/j.envexpbot.2010.05.006.

Borisova, Y., Minzagirova, A., Gilmanova, A., Galikhanov, F., Borisov, D., Yakubov, M., 2019. Heavy oil residues: application as a low-cost filler in polymeric materials. Civ. Eng. J. 5 (12), 2554–2568. https://doi.org/10.28991/cej-2019-03091432.

Centi, G., Perathoner, S., 2003. Catalysis and sustainable (green) chemistry. Catal. Today 77, 287–297. https://doi.org/10.1016/S0920-5861(02)00374-7.

Chattopadhyay, D.K., Webster, D.C., 2009. Thermal stability and flame retardancy of polyurethanes. Prog. Polym. Sci. 34 (10), 1068–1133. https://doi.org/10.1016/j.progpolymsci.2009.06.002.

Chen, Y.C., Chen, Y.H., 2019. Thermo and pH-responsive methylcellulose and hydroxypropyl methylcellulose hydrogels containing K_2SO_4 for water retention and a controlled-release water-soluble fertilizer. Sci. Total Environ. 655, 958–967. https://doi.org/10.1016/j.scitotenv.2018.11.264.

Chen, Y.C., Tai, W., 2018. Castor oil-based polyurethane resin for low-density composites with bamboo charcoal. Polymers 10 (10). https://doi.org/10.3390/polym10101100.

Chien, Y.C., Chuang, W.T., Jeng, U.S., Hsu, S.H., 2017. Preparation, characterization, and mechanism for biodegradable and biocompatible polyurethane shape memory elastomers. ACS Appl. Mater. Interfaces 9, 5419–5429. https://doi.org/10.1021/acsami.6b11993.

Dhaliwal, G.S., Anandan, S., Chandrashekhara, K., Lees, J., Nam, P., 2018. Development and characterization of polyurethane foams with substitution of polyether polyol with soy-based polyol. Eur. Polym. J. 107, 105–117. https://doi.org/10.1016/j.eurpolymj.2018.08.001.

Engels, H.W., Pirkl, H.G., Albers, R., Albach, R.W., Krause, J., Hoffmann, A., Casselmann, H., Dormish, J., 2013. Polyurethanes: versatile materials and sustainable problem solvers for today's challenges. Angew. Chem. Int. Ed. 52, 9422–9441. https://doi.org/10.1002/anie.201302766.

Gradinaru, et al., Ciobanu, C., Vlad, S., Bercea, M., Popa, M., 2012. Thermoreversible poly (isopropyl lactate diol)-based polyurethane hydrogels: effect of isocyanate on some physical properties. Ind. Eng. Chem. Res. 51 (38), 12344–12354. https://doi.org/10.1021/ie301690e.

Gurunathan, T., Mohanty, S., Nayak, S.K., 2015. Isocyanate terminated castor oil-based polyurethane prepolymer: synthesis and characterization. Prog. Org. Coating 80, 39–48. https://doi.org/10.1016/j.porgcoat.2014.11.017.

Gwon, J.G., Kim, S.K., Kim, J.H., 2016. Sound absorption behavior of flexible polyurethane foams with distinct cellular structures. Mater. Des. 89, 448–454. https://doi.org/10.1016/j.matdes.2015.10.017.

Hablot, E., Zheng, D., Bouquey, M., Avérous, L., 2008. Polyurethanes based on castor oil: kinetics, chemical, mechanical and thermal properties. Macromol. Mater. Eng. 293, 922–929. https://doi.org/10.1002/mame.200800185.

Hamilton, A.R., Thomsen, O.T., Madaleno, L.A.O., Jensen, L.R., Rauhe, J.C.M., Pyrz, R., 2013. Evaluation of the anisotropic mechanical properties of reinforced polyurethane foams. Compos. Sci. Technol. 87, 210–217. https://doi.org/10.1016/j.compscitech.2013.08.013.

Hejna, A., Kirpluks, M., Kosmela, P., Cabulis, U., Haponiuk, J., Piszczyk, Ł., 2017. The influence of crude glycerol and castor oil-based polyol on the structure and performance of rigid polyurethane-polyisocyanurate foams. Ind. Crop. Prod. 95, 113–125. https://doi.org/10.1016/j.indcrop.2016.10.023.

Huang, J., Zhang, L., 2002. Effects of NCO/OH molar ratio on structure and properties of graft-interpenetrating polymer networks from polyurethane and nitrolignin. Polymer 43, 2287–2294. https://doi.org/10.1016/S0032-3861(02)00028-9.

Huang, Y., Zhang, B., Xu, G., Hao, W., 2013. Swelling behaviours and mechanical properties of silk fibroin–polyurethane composite hydrogels. Compos. Sci. Technol. 84, 15–22. https://doi.org/10.1016/j.compscitech.2013.05.007.

Jhon, Y.K., Cheong, I.W., Kim, J.H., 2001. Chain extension study of aqueous polyurethane dispersions. Colloids Surf. Physicochem. Eng. Asp. 179, 71–78. https://doi.org/10.1039/C5RA27536A.

Jin, J.F., Chen, Y.L., Wang, D.N., Hu, C.P., Zhu, S., Vanoverloop, L., Randall, D., 2002. Structures and physical properties of rigid polyurethane foam prepared with rosin-based polyol. J. Appl. Polym. Sci. 84 (3), 598–604. https://doi.org/10.1002/app.10312.

Kashif, M., Ahmad, S., 2014. Polyorthotoluidine dispersed castor oil polyurethane anticorrosive nanocomposite coatings. RSC Adv. 4, 20984–20999. https://doi.org/10.1039/C4RA00587B.

Korley, L.T.J., Pate, B.D., Thomas, E.L., Hammond, P.T., 2006. Effect of the degree of soft and hard segment ordering on the morphology and mechanical behavior of semicrystalline segmented polyurethanes. Polymer 47, 3073–3082. https://doi.org/10.1016/j.polymer.2006.02.093.

Lang, J., Winkeljann, B., Lieleg, O., Zollfrank, C., 2019. Continuous synthesis and application of novel, archaeoinspired tackifiers from birch bark waste. ACS Sustain. Chem. Eng. 7, 13157–13166 (https://doi.org/).

Lee, W.J., Yu, C.Y., Chen, Y.C., 2018. Preparation and characteristics of polyurethane made with polyhydric alcohol-liquefied rice husk. J. Appl. Polym. Sci. 135, 45910. https://doi.org/10.1002/app.45910.

Lin, W.T., Lee, W.J., 2017. Effects of the NCO/OH molar ratio and the silica contained on the properties of waterborne polyurethane resins. Colloids Surf. Physicochem. Eng. Asp. 522, 453–460. https://doi.org/10.1016/j.colsurfa.2017.03.022.

Maiti, S., Ray, S.S., Kundu, A.K., 1989. Rosin: a renewable resource for polymers and polymer chemicals. Prog. Polym. Sci. 14, 297–338. https://doi.org/10.1016/0079-6700(89)90005-1.

Meier, M.A.R., Metzger, J.O., Schubert, U.S., 2007. Plant oil renewable resources as green alternatives in polymer science. Chem. Soc. Rev. 36, 1788–1802. https://doi.org/10.1002/chin.200805269.

Miao, S., Wang, P., Su, Z., Zhang, S., 2014. Vegetable-oil-based polymers as future polymeric biomaterials. Acta Biomater. 10, 1692–1704. https://doi.org/10.1016/j.actbio.2013.08.040.

Moustafa, H., El Kissi, N., Abou-Kandil, A.I., Abdel-Aziz, M.S., Dufresne, A., 2017. PLA/PBAT bionanocomposites with antimicrobial natural rosin for green packaging. ACS Appl. Mater. Interfaces 9 (23), 20132–20141. https://doi.org/10.1021/acsami.7b05557.

Mubofu, E.B., 2016. Castor oil as a potential renewable resource for the production of functional materials. Sustain. Chem. Processe. 4, 11. https://doi.org/10.1186/s40508-016-0055-8.

Mutlu, H., Meier, M.A.R., 2010. Castor oil as a renewable resource for the chemical industry. Eur. J. Lipid Sci. Technol. 112, 10–30. https://doi.org/10.1002/ejlt.200900138.

Ogunniyi, D.S., 2006. Castor oil: a vital industrial raw material. Bioresour. Technol. 97, 1086–1091. https://doi.org/10.1016/j.biortech.2005.03.028.

Petrović, Z.S., Zhang, W., Zlatanić, A., Lava, C.C., Ilavskyý, M., 2002. Effect of OH/NCO molar ratio on properties of soy-based polyurethane networks. J. Polym. Environ. 10, 5–12. https://doi.org/10.1023/A:1021009821007.

Santos, O.S.H., Coelho da Silva, M., Silva, V.R., Mussel, W.N., Yoshida, M.I., 2017. Polyurethane foam impregnated with lignin as a filler for the removal of crude oil from contaminated water. J. Hazard Mater. 324, 406–413. https://doi.org/10.1016/j.jhazmat.2016.11.004.

Schott, H., 1992. Swelling kinetics of polymers. J. Macromol. Sci. B 31, 1–9. https://doi.org/10.1080/00222349208215453.

Sehgal, P., Khan, M., Kumar, O., Vijayaraghavan, R., 2010. Purification, characterization and toxicity profile of ricin isoforms from castor beans. Food Chem. Toxicol. 48, 3171–3176. https://doi.org/10.1016/j.fct.2010.08.015.

Semsarzadeh, M.A., Navarchian, A.H., 2003. Effects of NCO/OH ratio and catalyst concentration on structure, thermal stability, and crosslink density of poly(-urethane-isocyanurate). J. Appl. Polym. Sci. 90 (4), 963–972. https://doi.org/10.1002/app.12691.

Sheldon, R.A., 2012. Fundamentals of green chemistry: efficiency in reaction design. Chem. Soc. Rev. 41 (4), 1437–1451. https://doi.org/10.1039/C1CS15219J.

Shi, L., Li, Z.M., Xie, B.H., Wang, J.H., Tian, C.R., Yang, M.B., 2006. Flame retardancy of different-sized expandable graphite particles for high-density rigid polyurethane foams. Polym. Int. 55 (8), 862–871. https://doi.org/10.1002/pi.2021.

Singhal, P., Rodriguez, J.N., Small, W., Eagleston, S., Van de Water, J., Maitland, D.J., Wilson, T.S., 2012. Ultra low density and highly crosslinked biocompatible shape memory polyurethane foams. J. Polym. Sci. B Polym. Phys. 50, 724–737. https://doi.org/10.1002/polb.23056.

Stanzione, M., Russo, V., Oliviero, M., Verdolotti, L., Sorrentino, A., Di Serio, M.,

Tesser, R., Iannace, S., Lavorgna, M., 2018. Characterization of sustainable polyhydroxyls, produced from bio-based feedstock, and polyurethane and copolymer urethane-amide foams. Data Brief 21, 269–275. https://doi.org/10.1016/j.dib.2018.09.077.

Tudorachi, N., Mustață, F., Bicu, I., 2012. Thermal decomposition of some Diels–Alder adducts of resin acids: study of kinetics process. J. Anal. Appl. Pyrolysis 98, 106–114. https://doi.org/10.1016/j.jaap.2012.07.013.

Vale, M., Mateus, M.M., Galhano dos Santos, R., Nieto de Castro, C., de Schrijver, A., Bordado, J.C., Marques, A.C., 2019. Replacement of petroleum-derived diols by sustainable biopolyols in one component polyurethane foams. J. Clean. Prod. 212, 1036–1043. https://doi.org/10.1016/j.jclepro.2018.12.088.

Wadekar, M., Eevers, W., Vendamme, R., 2019. Influencing the properties of Lignin PU films by changing copolyol chain length, lignin content and NCO/OH mol ratio. Ind. Crop. Prod. 141, 111655. https://doi.org/10.1016/j.indcrop.2019.111655.

Wang, C., Zheng, Y., Xie, Y., Qiao, K., Sun, Y., Yue, L., 2015. Synthesis of bio-castor oil polyurethane flexible foams and the influence of biotic component on their performance. J. Polym. Res. 22, 145. https://doi.org/10.1007/s10965-015-0782-7.

Wang, F., Wu, Z., Tanaka, H., 1999. Preparation and sizing mechanisms of neutral rosin size II: functions of rosin derivatives on sizing efficiency. J. Wood Sci. 45, 475–480. https://doi.org/10.1007/BF00538956.

Wang, J., Yao, K., Korich, A.L., Li, S., Ma, S., Ploehn, H.J., Iovine, P.M., Wang, C., Chu, F., Tang, C., 2011. Combining renewable gum rosin and lignin: towards hydrophobic polymer composites by controlled polymerization. J. Polym. Sci., Polym. Chem. Ed. 49, 3728–3738. https://doi.org/10.1002/pola.24809.

Wilbon, P.A., Chu, F., Tang, C., 2013. Progress in renewable polymers from natural terpenes, terpenoids, and rosin. Macromol. Rapid Commun. 34, 8–37. https://doi.org/10.1002/marc.201200513.

Yang, Y., Lin, Q., Huang, Y., Guo, D., 2011. Efficient preparation of mesocarbon microbeads by pyrolysis of coal-tar pitch in the presence of rosin. J. Anal. Appl. Pyrol. 91, 310–315. https://doi.org/10.1016/j.jaap.2011.03.005.

Zhang, J., Hori, N., Takemura, A., 2019. Optimization of preparation process to produce polyurethane foam made by oilseed rape straw based polyol. Polym. Degrad. Stabil. 166, 31–39. https://doi.org/10.1016/j.polymdegradstab.2019.05.022.

Zhang, L., Zhang, M., Zhou, Y., Hu, L., 2013. The study of mechanical behavior and flame retardancy of castor oil phosphate-based rigid polyurethane foam composites containing expanded graphite and triethyl phosphate. Polym. Degrad. Stabil. 98, 2784–2794. https://doi.org/10.1016/j.polymdegradstab.2013.10.015.

Zhang, M., Luo, Z., Zhang, J., Chen, S., Zhou, Y., 2015. Effects of a novel phosphorus–nitrogen flame retardant on rosin-based rigid polyurethane foams. Polym. Degrad. Stabil. 120, 427–434. https://doi.org/10.1016/j.polymdegradstab.2015.08.001.

Zhang, M., Pan, H., Zhang, L., Hu, L., Zhou, Y., 2014. Study of the mechanical, thermal properties and flame retardancy of rigid polyurethane foams prepared from modified castor-oil-based polyols. Ind. Crop. Prod. 59, 135–143. https://doi.org/10.1016/j.indcrop.2014.05.016.

Zhang, S., Xiang, A., Tian, H., Rajulu, A.V., 2018. Water-blown castor oil-based polyurethane foams with soy protein as a reactive reinforcing filler. J. Polym. Environ. 26, 15–22. https://doi.org/10.1007/s10924-016-0914-0.

Zhang, Y., Shang, S., Zhang, X., Wang, D., Hourston, D.J., 1995. Influence of structure of hydroxyl-terminated maleopimaric acid ester on thermal stability of rigid polyurethane foams. J. Appl. Polym. Sci. 58, 1803–1809. https://doi.org/10.1002/app.1995.070581019.

Zhang, Y., Shang, S., Zhang, X., Wang, D., Hourston, D.J., 1996. Influence of the composition of rosin-based rigid polyurethane foams on their thermal stability. J. Appl. Polym. Sci. 59, 1167–1171. https://doi.org/10.1002/(SICI)1097-4628(19960214)59:7<1167::AID-APP14>3.0.CO;2-2.

Zia, K.M., Bhatti, H.N., Ahmad Bhatti, I., 2007. Methods for polyurethane and polyurethane composites, recycling and recovery: a review. React. Funct. Polym. 67, 675–692. https://doi.org/10.1016/j.reactfunctpolym.2007.05.004.